Numerical and Experimental Study on Heat Transfer Enhancement by Vortex Generation

Prof. Dr. Jalal M. Jalil
Educational Technology Department
University of Technology, Baghdad, Iraq

Prof. Dr. Khalid A. Ismeal
Mechanical Engineering Department
University of Technology, Baghdad, Iraq

Asst. Prof. Dr. Sabah T. Ahmed
Mechanical Engineering Department
University of Technology, Baghdad, Iraq

Abstract

Numerical and experimental study was carried out on heat transfer enhancement using a slender delta wing vortex generator to generate longitudinal vortices in a rectangular duct. Numerically, laminar with constant wall temperature was considered. Effect of angle of attack of the wing (from 0.0 to 56.5 degree) on the Spain-wise average Nusselt number and the span wise average skin friction coefficient were investigated. Numerical results demonstrate similar behavior to the published results of other investigators.

Experimentally, effect of angle of attack (from 0.0 to 56.5 degree) of the vortex generator, wing aspect ratio of the vortex generator (from 0.5 to 2.0) and wing width to duct width (from 0.25 to 0.5) on the heat transfer process for laminar flow (Re = 750 to 2700) and turbulent flow (Re = 4100 to 7950) were investigated. Both numerical and experimental results show the enhancement of heat transfer but experimental results show higher values of Nusselt number compared with the numerical results.

الخلاصـــة

تم في هذا البحث إجراء دراسة عددية و عملية حول تحسين انتقال الحرارة باستخدام مولد دوامات نحيف على شكل جنيح مثلث لتوليد دوامات طولية في مجرى مستطيل المقطع. عدديا استخدم مجرى طباقي مع جدران درجة حرارتها ثابتة. وقد تم دراسة تأثير زاوية الهجوم لمولد الدوامات من صفر إلى 56.5 إلى المتوسط العرضي لرقم نسلت وكذلك المتوسط العرضي لمعامل احتكاك السطح. وقد أوضحت الدراسة العددية تصرف مشابه لما نشره الباحثون الآخرون.

عمليا تم دراسة تأثير زاوية الهجوم من صفر إلى 56.5 درجة ونسبة عرض الجنيح إلى عرض المجرى من 0.25 إلى 0.5 لجريان الطباقي (بيتراوح عدد رينولدز بين 750 إلى 2700) ولجريان مضطرب (بيتراوح عدد رينولدز بين 4100 و 7950). وقد أظهرت كلا النتائج العملية و النظرية زيادة في انتقال الحرارة ولكن النتائج العملية أظهرت قيم لنسلت أعلى من النتائج العددية.

1. Introduction

Compact heat exchangers are being used increasingly in industrial applications. On the gas side the flow is laminar forced and thermal resistance is still the dominant resistance in such heat exchangers. Reduction of this thermal resistance will reduce heat transfer area and so that costs of heat exchanger will be lower [1,2]. Downstream of the duct or channel the heat transfer coefficient is low due to thicker boundary layer, so that augmentation of heat transfer is important. Augmentation techniques usually employ fins, ribs or vortex generators attached to the heat transfer surfaces to provide additional surface area for heat transfer, controlling boundary layer growth and improve mixing which leads to higher heat transfer rate.

Comprehensive survey of the literature on heat transfer and friction losses for the flow through channels and duct was done [2-5], also experimental and numerical studies [6,7] were done for heat transfer augmentation techniques. One of the augmentation techniques is a slender delta wing or winglets vortex generator, this will generate longitudinal vortices along the side edge of the wing due to pressure difference between the front surface facing the flow and the back surface, these vortices will increase mixing and enhance heat transfer rate, but at the same time increase pressure losses. From theory and experimental work [8-10] it was found that the slender delta wing gives the best results.

In the present study a numerical and experimental study on a laminar flow in a rectangular duct containing a single built-in slender delta wing vortex generator was done.

2. Numerical Model

The mathematical formulation of the fluid flow problems is governed by basic conservation principles namely the conservation of mass (continuity equation), momentum (Navier-Stokes equation) and energy equation. In this investigation the airflow was a three-dimensional steady state incompressible laminar flow through a rectangular duct with a delta wing vortex generator. Numerical modeling of airflow was done using finite difference methods, which offer simplicity to numerical solution of partial, non-linear differential equations (34, 35). Numerical solution of the non-dimensional basic governing equation was done using the staggered grid in which all the scalar dependent variables are stored at the main grid points, but the velocity component are stored at "staggered grid" (the points lie on the faces of the control volumes). Some physically unrealistic fields will arise as solution, if the velocity components and pressure are calculated for the same grid point. These difficulties are discussed fully in Patanker [4]. The upwind scheme is adopted in the present study for the solution of the discritized equations generated from the finite difference solution of the basic non-dimensional equations governing the flow field

In the theoretical model the effect of entrance region was neglected and a uniform flow through the duct was presented with constant walls temperature. The vortex generator of negligible thickness was considered perfectly conductive and flow at the exit was considered smooth.

Computation is performed in a rectangular duct **Fig.(1)**. For detailed investigations, only one delta wing (of zero thickness) is placed inside the duct as a vortex generator. The base of

the wing is fixed at the bottom wall and the apex faces the incoming stream, with an angle of attack. The dimensionless equations for incompressible without buoyancy, continuity, momentum and energy may be expressed in the following conservative forms:
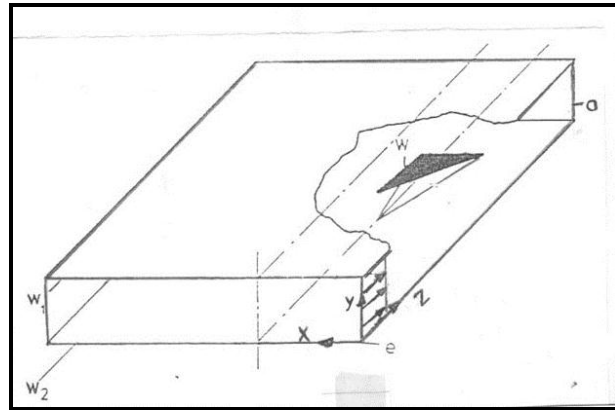
Figure (1) Computational Domain with Boundary Condition as Fallows: e: Entrance; a: Exit, w1and w2: Upper and Lower Walls with No-Slip Condition

$$\frac{\partial U}{\partial X} + \frac{\partial V}{\partial Y} + \frac{\partial W}{\partial Z} = 0.0 \quad \text{...} \quad (1)$$

$$\frac{\partial U^2}{\partial X} + \frac{\partial UV}{\partial Y} + \frac{\partial UW}{\partial Z} = -\frac{\partial P}{\partial X} + \frac{\nabla^2 U}{Re} \quad \text{.....................................} \quad (2)$$

$$\frac{\partial VU}{\partial X} + \frac{\partial V^2}{\partial Y} + \frac{\partial VW}{\partial Z} = -\frac{\partial P}{\partial Y} + \frac{\nabla^2 V}{Re} \quad \text{.....................................} \quad (3)$$

$$\frac{\partial WU}{\partial X} + \frac{\partial WV}{\partial Y} + \frac{\partial W^2}{\partial Z} = -\frac{\partial P}{\partial Z} + \frac{\nabla^2 W}{Re} \quad \text{.....................................} \quad (4)$$

$$\frac{\partial U\theta}{\partial X} + \frac{\partial V\theta}{\partial Y} + \frac{\partial W\theta}{\partial Z} = \frac{\nabla^2 \theta}{Re.Pr} \quad \text{.....................................} \quad (5)$$

where:

$$U = \frac{u}{W_{in}}, \qquad V = \frac{v}{W_{in}}, \qquad W = \frac{w}{W_{in}}$$

$$X = \frac{x}{dh}, \qquad Y = \frac{y}{dh}, \qquad Z = \frac{z}{dh}$$

$$t = \frac{\tau.W_{in}}{dh}, \qquad\qquad P = \frac{p}{\rho.W_{in}^2}, \qquad\qquad Re_z = \frac{W_{in}.dh}{v}$$

$$\theta = \frac{T - T_{ia}}{T_w - T_{ia}}, \qquad\qquad Re_z = \frac{\rho.W_{in}.dh}{\mu}, \qquad\qquad Pr = \frac{C_p.\mu}{k}, \qquad\qquad Pe = Re_z.Pr$$

Staggered grid arrangements are used in which velocity components are defined at the cell faces to which they are normal **Fig.(2)**. The pressure and temperature are defined at the center of the cell. In order to state further details about the kinematics conditions on the wing, specific discussion can be made with the help of **Fig.(3)**. The axial and normal components of velocity which fall directly on the wing are set to zero. Span wise components do not fall is interpolated on the wing from neighboring cells and then the interpolated velocity components are set equal to zero.
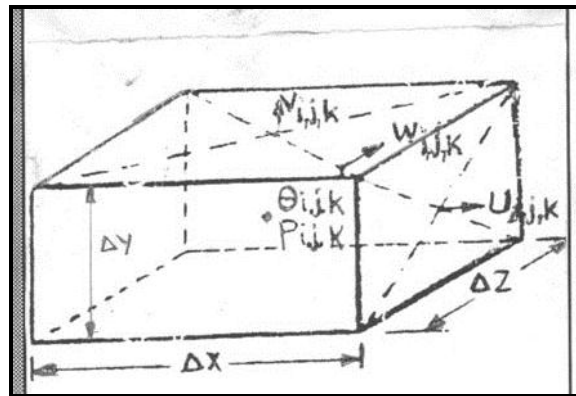
Figure (2) Three-Dimensional Staggered Grid Showing the Location of the Discritized Variables
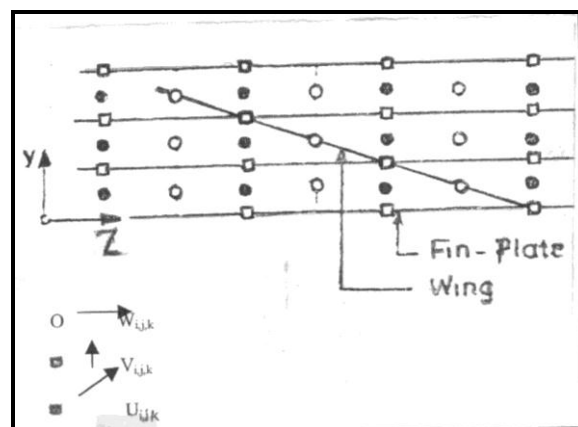
Figure (3) Relative Location of Velocity Components on the x-z Plane at the Middle of the Duct

2-1 Boundary Conditions

At wall surfaces and at obstacle:

The velocity components at all the duct walls and obstacle are equal to zero, because of the viscous nature of the flow:

$U = V = W = 0$

The temperatures of the duct walls and the obstacle are the same so that : $T = T_w$

At Inlet:

$U = V = 0$

$W = W_{in}$; uniform

$\theta = \theta_{in}$; uniform

$p = p_{in}$; uniform

At Exit:

At exit, a smooth transition through the outflow boundary is ensured by setting the second partial derivative of the three components of the exit velocity is set equal to zero.

The finite difference form of the second derivative of the variable (ϕ) in the flow direction (X-direction) which is affected by three preceding nodes is:

$$\frac{\partial^2 \phi}{\partial x^2} = \frac{-5\phi_{i,j,k-3} + 4\phi_{i,j,k-2} - \phi_{i,j,k-1} + 2\phi_{i,j,k}}{\Delta x^2} \quad \text{.. (6)}$$

where:

  i : represents the node position in the x-direction.

  j : represents the node position in the y-direction.

  k : represents the node position in the z-direction.

The discretization equation based on the differential equations (1), (2), (3), and (4) can easily be seen to be:

$$A_P \Phi_P = A_E \Phi_E + A_W \Phi_W + A_N \Phi_N + A_S \Phi_S + A_T \Phi_T + A_B \Phi_B + S_P \text{ .... (7)}$$

$$A_P = A_E + A_W + A_N + A_S + A_T + A_B \text{ .... (8)}$$

At this point, it is interesting to examine the physical significance of the various coefficients in the discretization equations. The neighbor coefficients (A_E, A_W, A_N, A_S, A_T, A_B) represent the connective between the point (P) and the corresponding neighbor. The center point coefficient (A_P) is the sum of all neighbor coefficients. But the term (S_P) is the pressure difference source for momentum equations only.

3. Experimental Investigation

It was found necessary to make an experimental investigation because of the shortage in published literature on experimental work compared with the numerical one, also to find out the relation between experimental and numerical results in this investigation. A test rig was built in this investigation which consisted of rectangular duct of (10 x 20 cm) cross sectional area and about (425 cm) in length supplied with a delta wing vortex generator, this rig formed a part of an open wind tunnel.

Figure (4) shows the schematic of the experimental rig which can be considered as an open wind tunnel which consists basically of four sections, which are:

1. The heating section (heating power 2350 watts).
2. The damping section.
3. The test section.
4. The draft section.

This test section was (100 cm) in length; ten stations were used to measure the temperature difference between the wall and the air layer adjacent to the wall (about 5 mm away from the wall). Five of these ten stations had six points for measuring temperature difference and only one point along the centerline of the bottom wall of the other five stations. In each station these six points are distributed on the bottom wall and side wall at equal distance starting from the centerline of the bottom wall, three of these points on the bottom wall and the other three on the side wall. Each station represents half of the duct and by assuming symmetric temperature distribution in each station; these six temperature points represent the temperature distribution for all the walls of the plane at that station which was perpendicular to the direction of airflow. **Figure (5)** shows a schematic diagram for this section and the positions of the stations.

Many vortex generators were manufactured from galvanized steel sheet, these vortex generators can be classified mainly in three groups:

1. Vortex generators of constant wing aspect ratio (Λ) and ratio of wing span to width of the channel (Br) with different angles of attack (β).
2. Vortex generators of constant wing aspect ratio and angles of attack with different (Br).
3. Vortex generators of constant (Br) and angle of attack with different wing aspect ratios.

Hot air of controlled temperature was supplied to the duct and heat transfer rate was measured in test section of about (100 cm) in length by measuring temperature differences of the walls using thermocouples-wires. The program of tests included laminar flow tests and turbulent flow tests. The parameters investigated were angle of attack of the wing (β), Reynolds number, wing aspect ratio (Λ) and ratio of width of the wing to width of the duct (Br). **Figure (6)** shows different samples of vortex generators with different dimensions, which were used, in this experimental investigation.
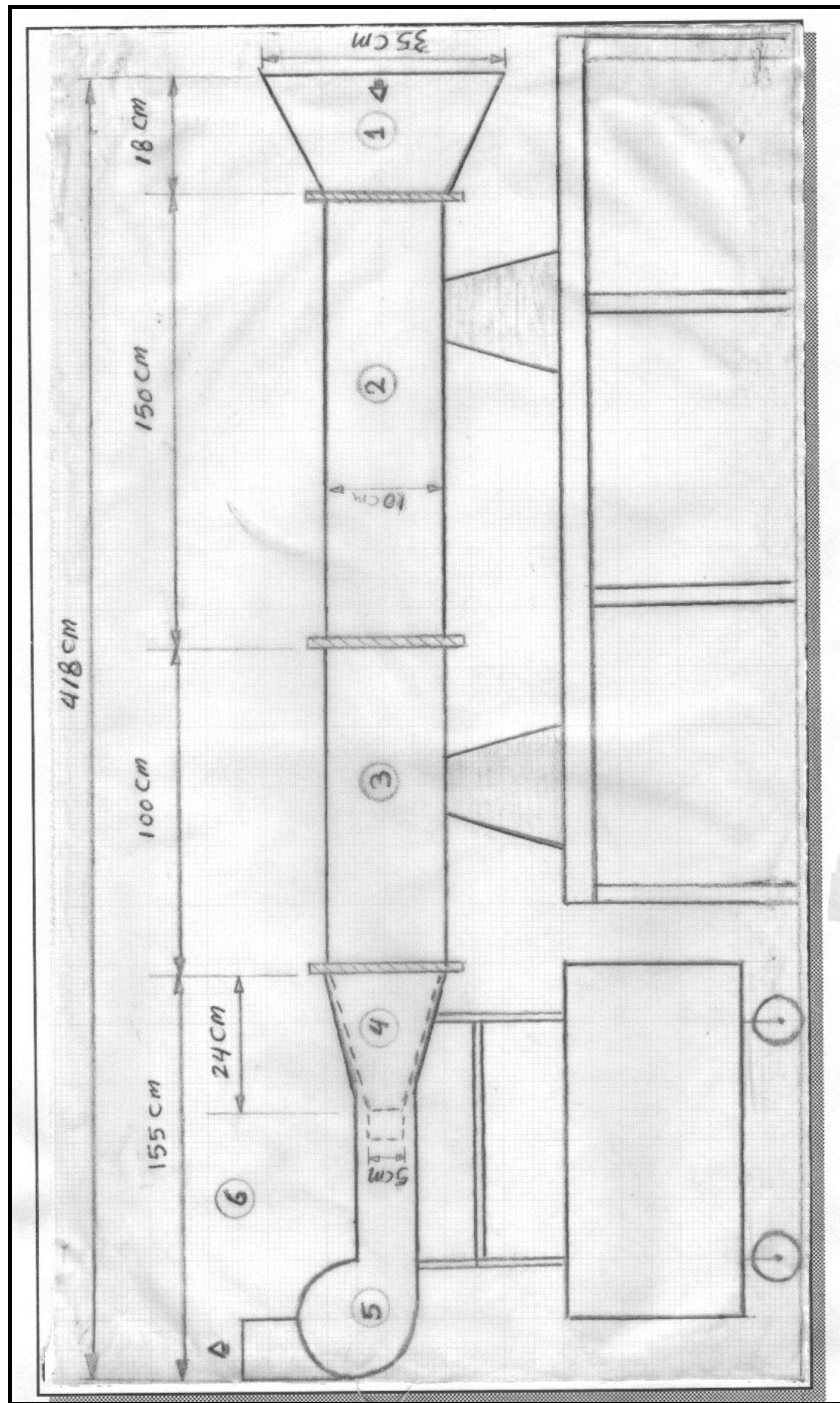
Figure (4) Schematic Diagram of the Experimental Rig.
1. Heating Section, 2. Damping Section, 3. Test Section,
4. Fitting Section, 5. Centrifugal Fan, and, 6. Draft Section
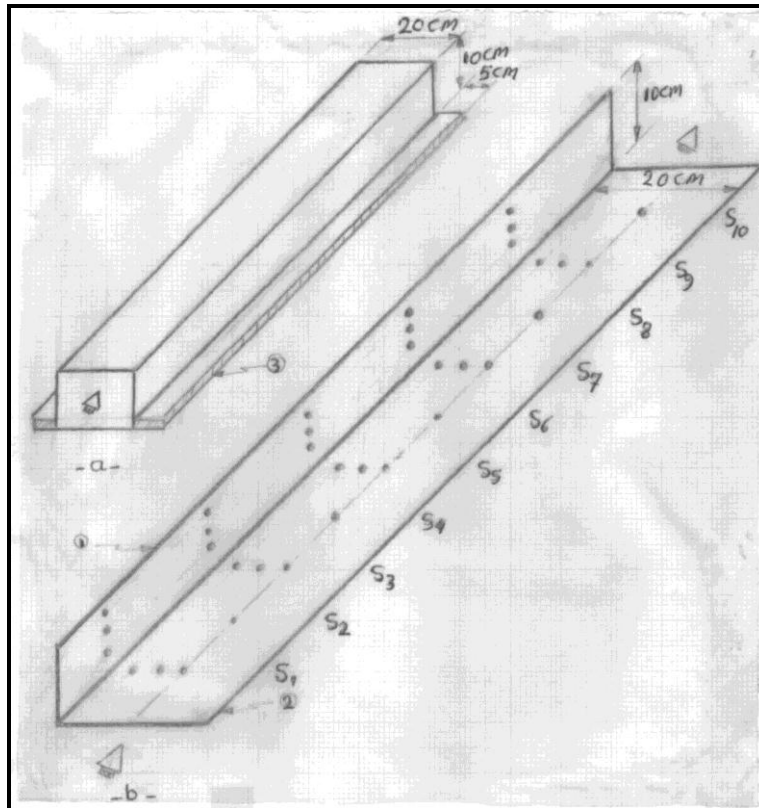
Figure (5) Schematic Diagram of the Test Section
a. Overall Look of the Section, b. Position of Thermocouple which are
Distributed at Equal Distances on the Half of the Test Section,
1. Side Wall, 2. Bottom Wall, 3. Plastic Gasket, S. Station
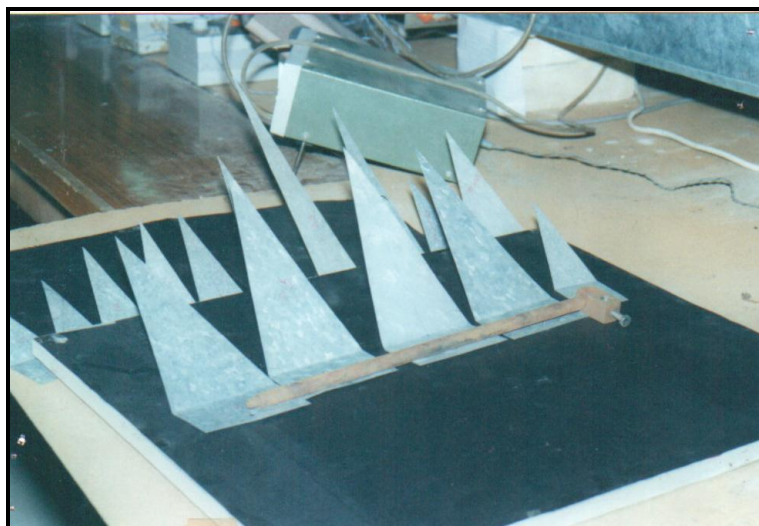
Figure (6) Different Types of Vortex Generation

4. Results and Discussion

4-1 Numerical Results

A computer program was build by the author applying the finite volume using SIMPLE algorithm [4]. One slender wing-type vortex generator of negligible thickness with an angle of attack to the direction of cooled airflow was put in the duct constant wall temperature (hot wall). Computation was performed for this case with different angle of attack and different Reynolds numbers. The result of the computations covered the flow field (U, V and W), thermal field (temperature distribution) and heat transfer enhancement (Nusselt Number) through the duct due to the existence of the wing-type vortex generator.

A large number of computations have been performed at different Reynolds numbers and angle of attack (β) with a delta wing as a wing generator. **Figure (7)** shows a typical picture of the longitudinal velocity vectors at the mid plane on a longitudinal section of the duct fir different Reynolds numbers (100, 500 and 1000) for an angle of attack (β=45) and Prandtl = 0.72. A spiraling structure of the main flow is discern behind the wing it is seen that the magnitude of the velocity vectors for the case of Re=100 is less than that for case with Re=500, and this is less than for the case with Re=1000. This observation is made through the comparison of velocity vectors at the axial location in these cases; this is due to higher momentum so those stronger vortices occur as Reynolds number increases.

The wing-type vortex generator will induce streetwise longitudinal vortices behind it and as shown from **Fig.(7)** the longitudinal vortices will persist in an area which is many times larger than the wing area and continue behind the wing to a distance many times larger than the wing span (l).

Figures (8) and **(9)** show a typical picture of the generation of vortices and their gradual growth as moving downstream in the duct, then deformation of the vortices start as they move deeply in the duct due to viscosity of the walls. **Figure (8)** shows the cross-stream velocity vectors at different axial locations of the duct for Re = 500, β = 45). This figure illustrate no vortices before the wing, then generation of the vortices starts at the wing at location z = 0.2, then its growth continues behind the vortex generator as shown in **Fig.(9)**. As mentioned before the wing will induce longitudinal vortices behind it, which will take the fluid from the underside of the wake and swirl it around to the upper side, entraining fluid from the periphery to the center of the vortices. This mechanism will finally culminate in the disruption of the growth of the thermal boundary layer and the heat transfer coefficient will be enhanced.

Figure (10) show the growth of isotherms for thermally and hydro-dynamically developed duct flows with a built-in delta wing at progressive distance along the duct, for Reynolds number 100, 500 and 1000, for deltas wing vortex generator with 45 degree angle of attack. The wing has the same constant temperature as the walls. For the simple duct flow (the base flow before the wing) the isotherms are straight lines along y/h = constant, and the thermal boundary layer is evident at section where z= 0.1, the vortex generator distorts this temperature field strongly. In the wing tip region the vortices suck flow velocity fluid into the

vortex and come close to the wing, which leads to a thickening of the temperature boundary layer downstream of the wing base on the wall opposite the base plate. On the base plate behind the wing the velocity gradient are higher than those in the surrounding area, and the isotherms are close together. Behind the wing the temperature disturbances are convicted over the whole cross-section by the cross-flow. The isotherms are spaced wider except near the wing symmetry plane close to the wall, where the wing is attached, and near the array symmetry plane close to the opposite wall.
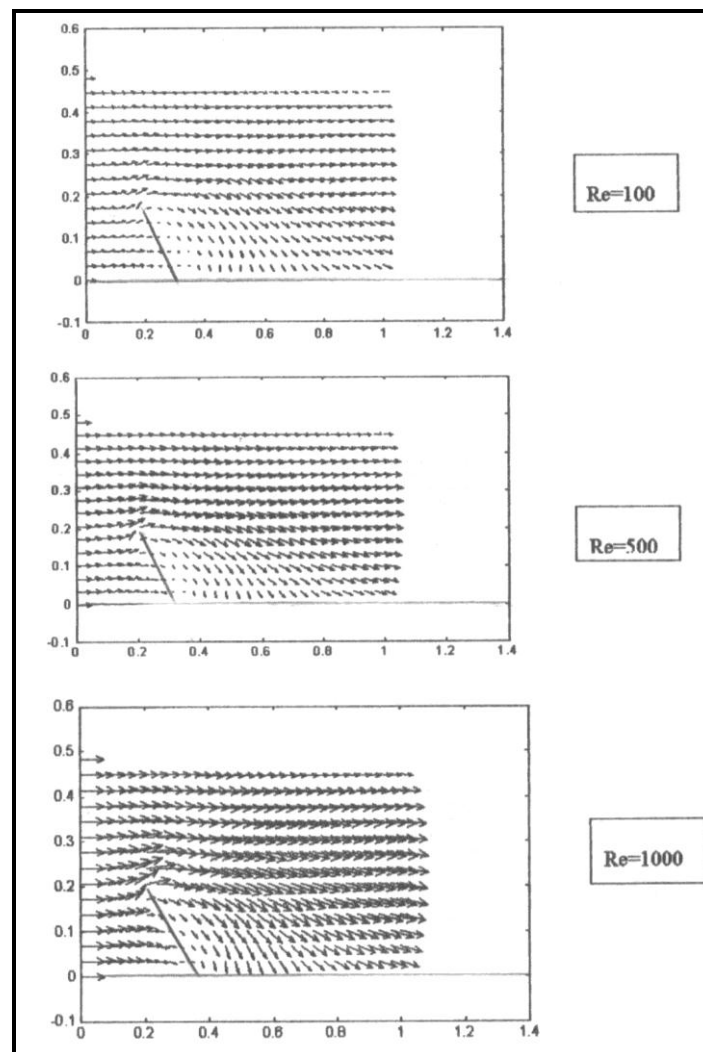
Figure (7) Longitudinal Velocity Vectors at the Mid Plane (x=0.5) for a Duct with a Delta Wing Vortex Generation, (Fixed from z=0.2 to 0.366) for Different Reynolds Numbers and Angle of Attack β=45 Degree
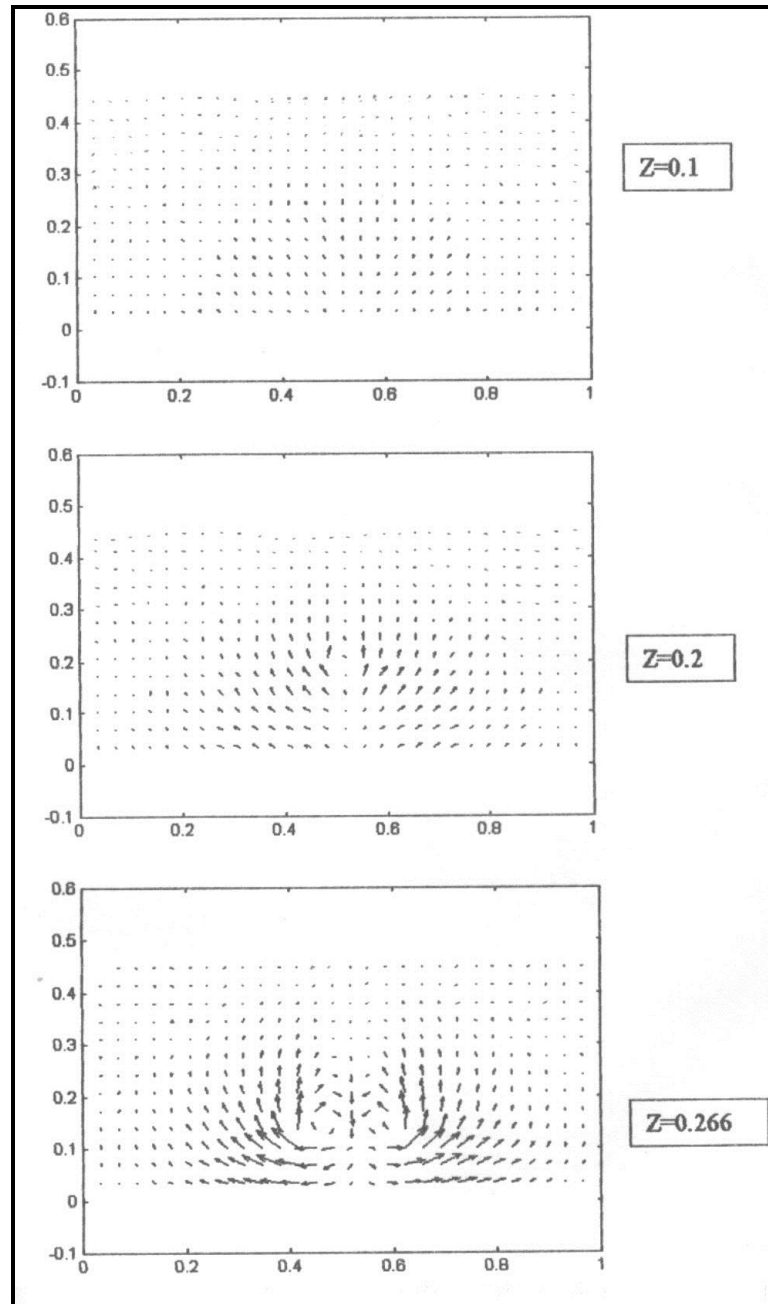
Figure (8) Cross-Stream Velocity at Different Axial Location before and Through the Wing Showing Generation and Growth of Vortices in the Channel for Re=500 and Angle of Attack β=45 Degree
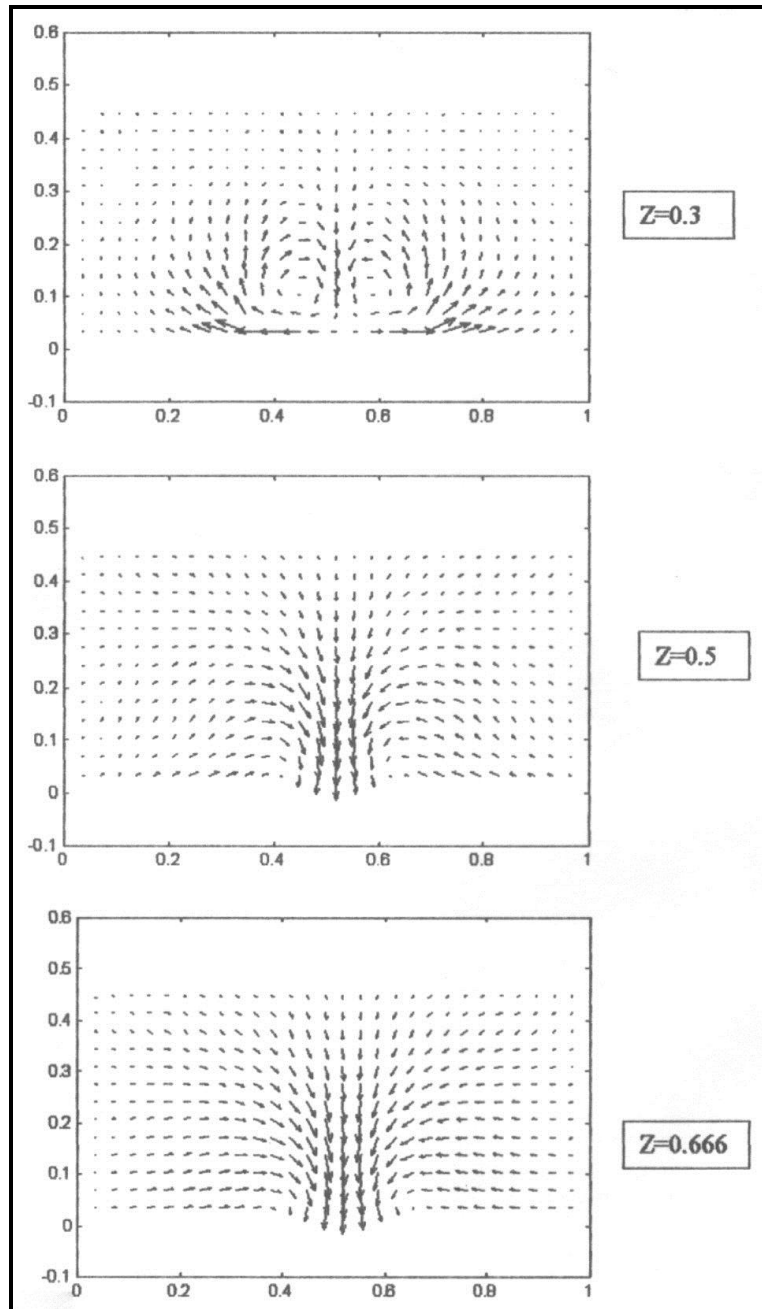
**Figure (9) Cross-Stream Vectors at Different Axial Locations
Through and Growth of Vortices in the Channel for Re=500
and Angle of Attack β=45 Degree**
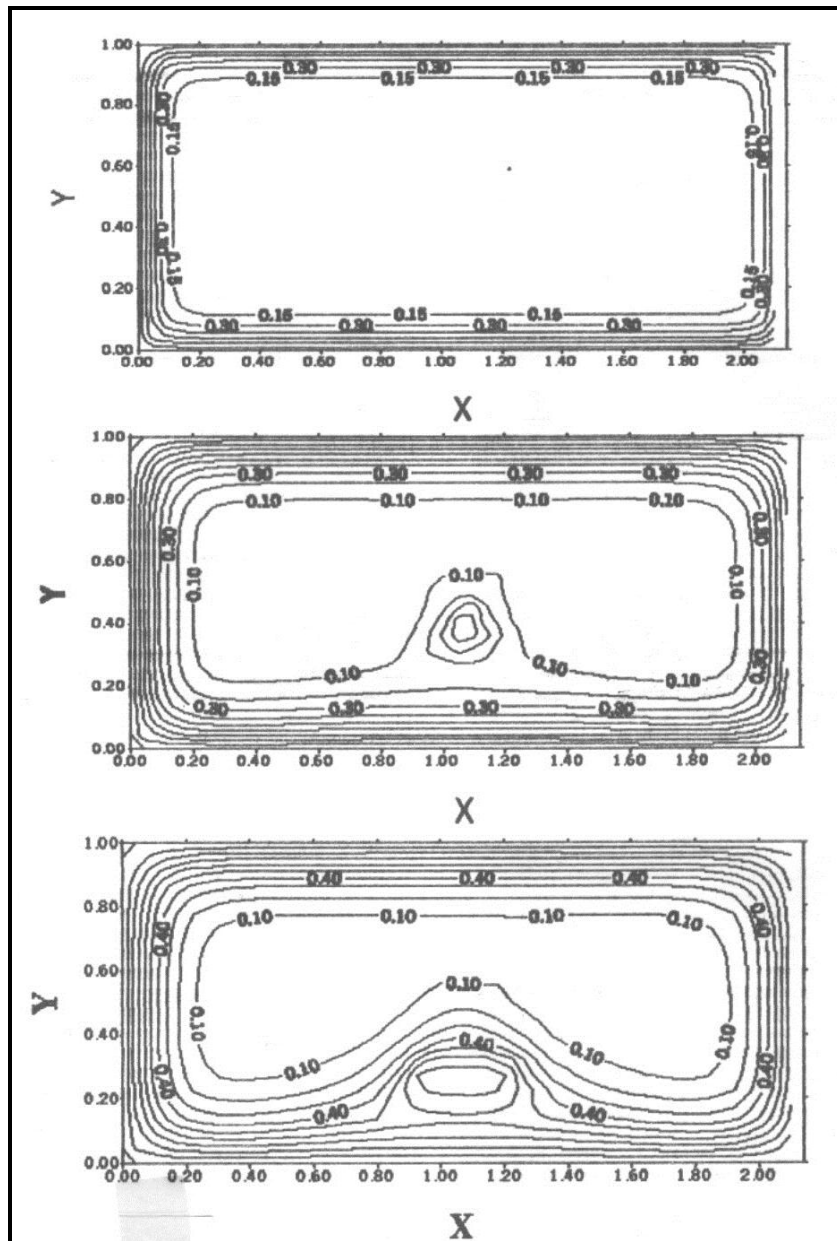
**Figure (10 a) Isothermal Contour for a Flow through a Duct
with a Delta Wing Vortex Generation for Re=100,
at Progressive Distances z= 0.1, 0.2, 0.266**
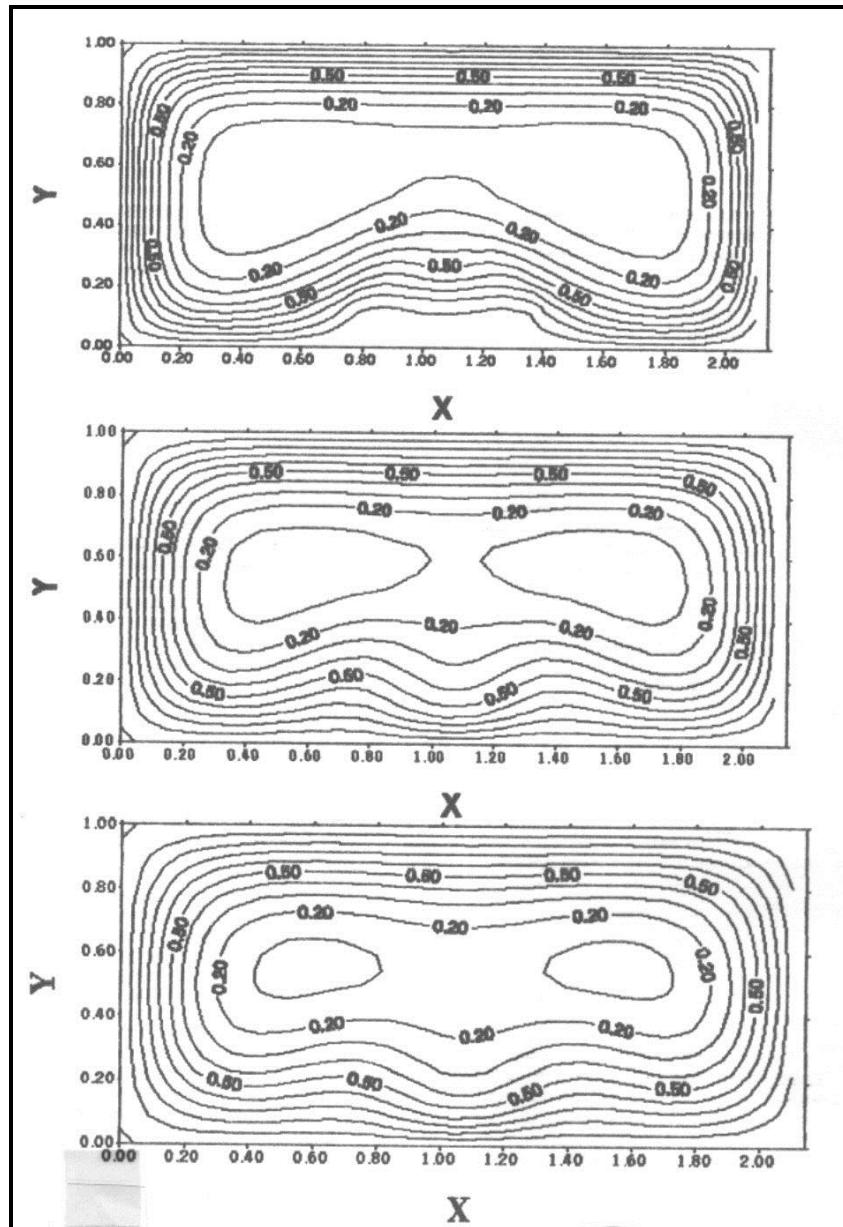
**Figure (10 b) Isothermal Contour for a Flow through a Duct
with a Delta Wing Vortex Generation for Re=100,
at Progressive Distances z= 0.3, 0.5, 0.66**

   Figures (11) and **(12)** show the variation of combined span-wise average Nusselt along the duct for smooth flow for different Reynolds numbers. It is clear that Reynolds number increases the value of combined span-wise average Nusselt number increases, this is because a higher Reynolds number signifies a higher mass flow rate and as a consequence a higher heat removal rate is observed.
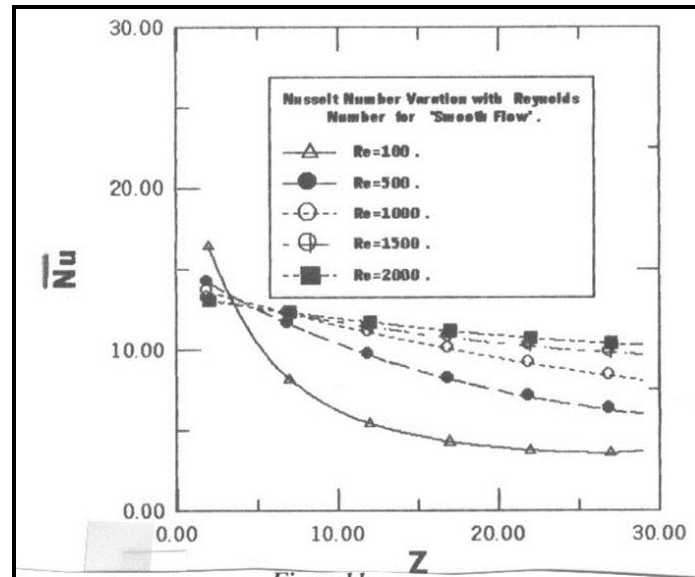
Figure (11) Variation of Combined Span Wise Average Nusselt Number along a Duct for Smooth Flow for Different Reynolds Numbers
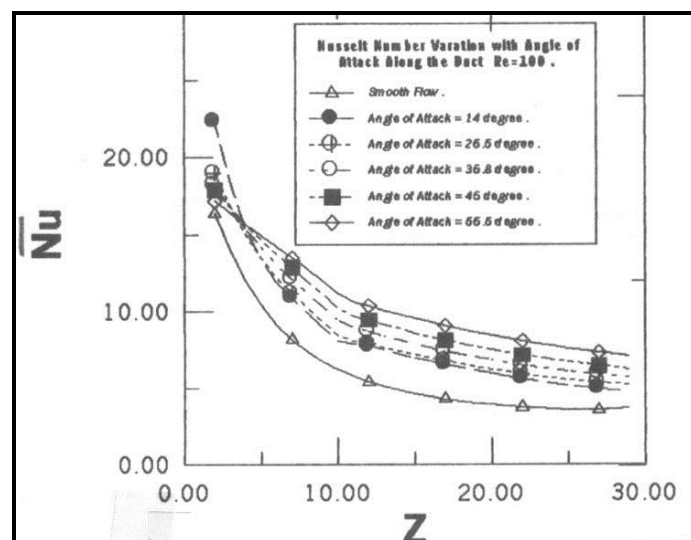
Figure (12) Effect of Angle of Attack on Distribution of Combined Span Wise Average Nusselt Numbers along the Duct for Smooth Flow with Vortex Generator, for Re=100

In order to examine the influence of angle of attack of the delta wing vortex generator on heat transfer we observe **Fig.(12)**. It is observed that the combined span-wise average Nusselt number increases with increasing angle of attack. Wings with higher angles of attack produce vortices with higher strength which result in better heat transfer, because increasing angle of attack will make the wing in contact with the fluid of higher momentum which is near the free stream away from the wall. In the region of the wing, the combined span-wise average Nusselt number rises to a high value up to a region behind the span-wise average Nusselt number rises to a higher value up to a region behind the middle of the wing and then takes a plunge. A small dead water zone exists in the immediate neighborhood behind the wing-body junction that eventually causes poor heat transfer at that location.

For **Fig.(12)** combined span-wise average Nusselt number reduces as they move along the duct due to the deformation of the vortices as moving away from the wing. Deformation occurs due to the reduction in strength of the vortices, which is brought about by the viscous resistance of the walls.

4-2 Experimental Results

The experimental results were plotted between the combined span-wise average Nussult number ($\overline{Nu}$) and the distance along the duct. Values of Reynolds number for laminar flow test set varied from (Re = 450 up to 2750) while for turbulent flow from (Re = 4367 up to 7945), angle of attack of the vortex generator (β) was changed from ($\beta = 14\overset{\circ}{}$ up to $\beta = 56.5\overset{\circ}{}$), wing aspect ratio ($\Lambda$) from ($\Lambda = 0.5$ up to 2.0) and (Br) from (Br = 0.25 up to 0.50).

The experimental results show nearly the same expected behavior obtained from numerical results, with some differences, but the experimental values of ($\overline{Nu}$) were higher than that expected from theoretical model especially downstream the duct. The experimental results for laminar flow were correlated and a final equation of ($\overline{Nu}$) as a function of Reynolds number, location through the duct, and angle of attack of the wing was obtained which gives higher values of ($\overline{Nu}$) when compared with the numerical one. For turbulent flow only equations predict values of ($\overline{Nu}$) as a function of Reynolds number for each location through the duct for two angles of attack of the wing (β) which are ($\beta=14^{o}$ and $\beta=45^{o}$) and which were correlated.

Many different experiments were done on laminar and turbulent flow with, and without vortex generator for different angles of attack (β) and different Reynolds numbers (Re). Effect of different wing aspect ratios (Λ) and effect the ratio of wing width to duct width (Br) for laminar flow were also investigated, these tests can be summarized as follows: the specifications of the vortex generator and flow are recorded in **Tables (1, 2, 3)**.

Table (1) Specification of Vortex Generator and Flow for Different Wing Aspect Ratio (Λ) Test No.10

	Run. No.1	Run. No.2	Run. No.3	Run. No.4
β	45°	45°	45°	45°
ℓ	5 cm	10 cm	15 cm	20 cm
B	5 cm	5 cm	5 cm	5 cm
Λ	2.0	1.0	0.75	0.5
Re	1000	1000	1000	1000

Table (2) Specification of Vortex Generator and Flow for Different (Br), Test No.11

	Run. No.1	Run. No.2	Run. No.3
β	45°	45°	45°
ℓ	20 cm	15 cm	10 cm
B	10 cm	7.5 cm	5 cm
Λ	1.0	1.0	1.0
B	20 cm	20 cm	20 cm
Re	1009	1009	1009
Br	0.5	0.375	0.25

Table (3) Specification of Vortex Generator and Flow for Turbulent Flow Investigation

	Test No.12	Test No.13	Test No.14
β	Different angle	45°	45°
ℓ	20 cm	20 cm	20 cm
b	10 cm	10 cm	10 cm
B	20 cm	20 cm	20 cm
Br	0.5	0.5	0.5
Re	5045	Different Re	Different Re

Figure (13) shows the effect of angle of attack of the wing for turbulent flow with constant specification and Re=5045. It is clear that increasing angle of attack will cause heat transfer enhancement by increasing Nu. This is because increasing angle of attack will make the original vortices due to turbulent flow stronger by making the tip of the wing in contact with the fluid of higher momentum, which is away from the wall. **Figures (14)** and **(15)** show the variation in Log Nu with Log Re for laminar flow at different locations along the duct, for different angles of attack of the vortex generator (56.5, 14 degrees respectively). There is an equation for each curve. It is representing the value of Nu as a function of Re at each location along the duct has the form of Nu = c Re^m, the values of (c and m) for each curves can be obtained easily from the figures. The same thing is done for turbulent flow test as shown in **Fig.(16)**. The final equation which describes Nu as a function of Re, z, and β.

$$Nu = C \, Re^m \, Z^n \, \beta^k \quad \text{.. (9)}$$

where, C = 1.3951, m = 0.306, n = 0.1535, k = -0.049059

This equation was tested numerically and it gives reasonable results compared with the numerical and experimental results in this investigation. **Figure (16)** gives comparison between the results in this investigation and those of Biswas [8]. In this theoretical model of this investigation the value of Λ is equal to 4 while Biswas in his experimental investigation Λ is equal to 1 but the values of β, Re, Br and α are the same, good agreement was observed.
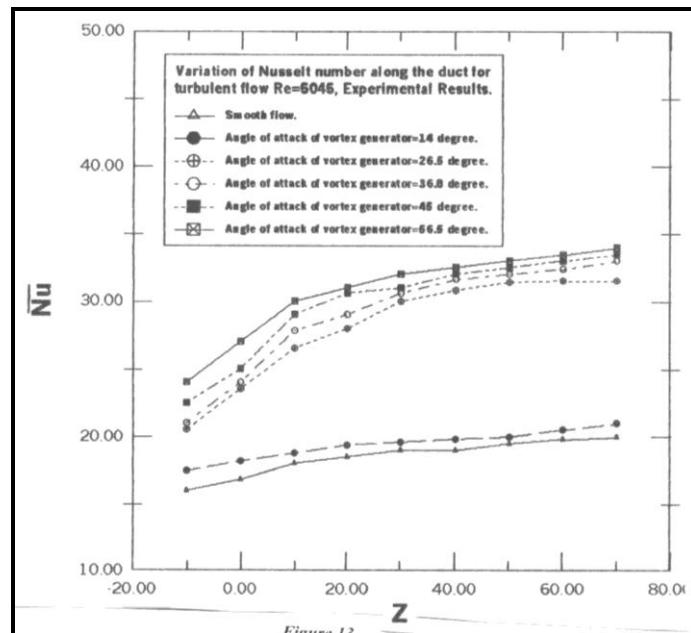
Figure (13) Effect of Angle of Attack of Vortex Generation on the Distribution of Nusselt Numbers along the Duct for Turbulent Flow Re= 5045, b=10, and l= 20cm and br= 0.5
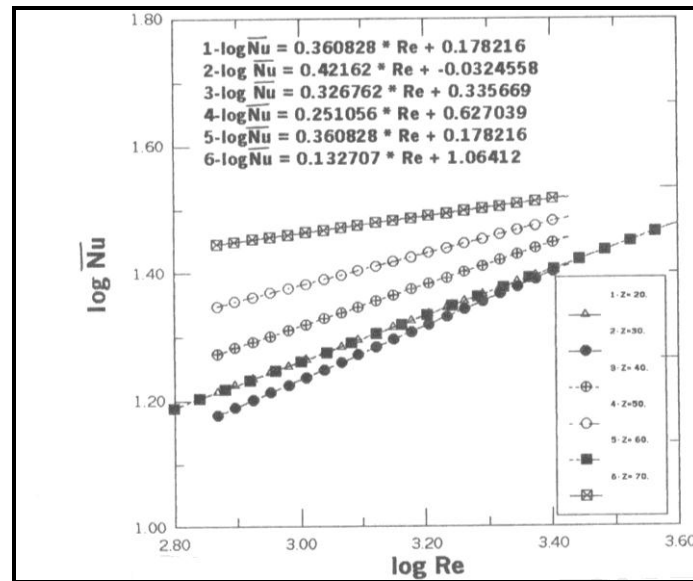
Figure (14) Variation of Log Nu with Log Re for Different Location along the Duct with a Delta Wing Vortex Generator of 56.5 Degree Angle of Attack, Laminar Flow, Experimental Results
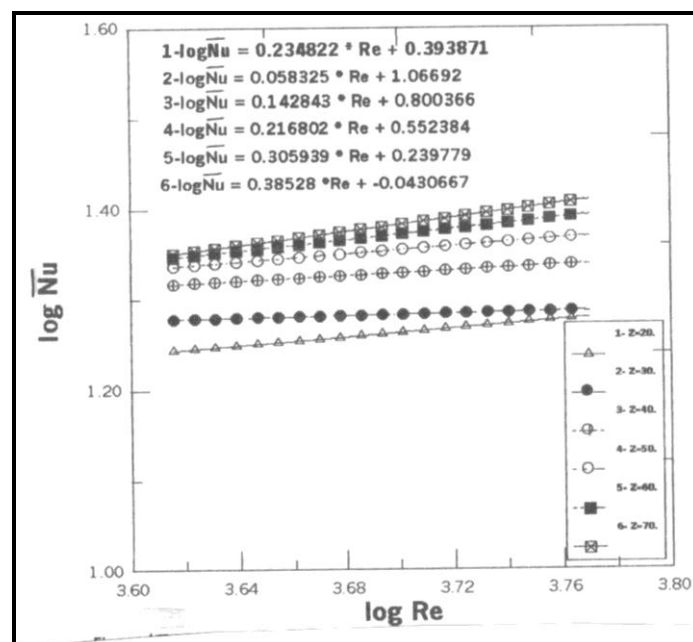
Figure (15) Variation of Log Nu with Log Re for Different Location along the Duct with a Delta Wing Vortex Generator of 14 Degree Angle of Attack, Turbulent Flow, Experimental Results
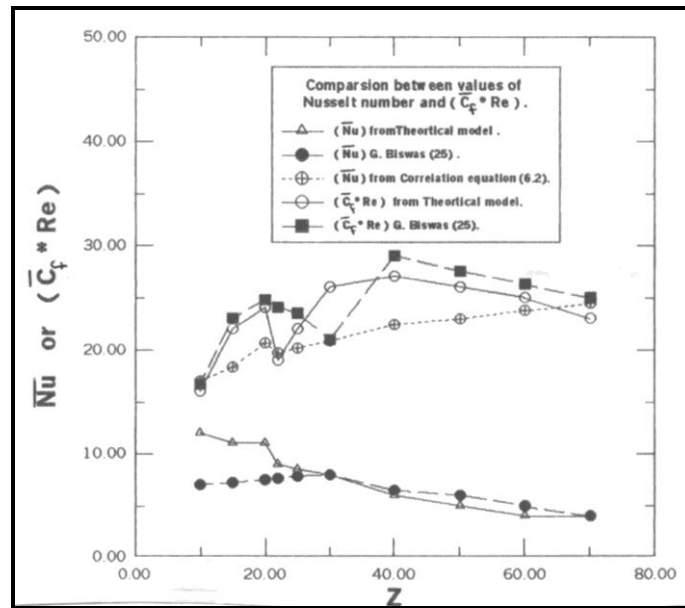
Figure (16) Comparison between Values of Nusselt Number along the Duct with a Delta Wing Vortex Generator of 26 Degree Angle of Attack, Re= 500, Wing Aspect Ratio 1, br= 0.5, j2

5. References

1. M., Fiebig, U., Brackmeier, N. K., Mitra, and T. Giintermann, *"Structure of Velocity and Temperature Field in Laminar Channel Flow with Longitudinal Vortex Generators"*, Numerical Heat Transfer, Part A, Vol. 15, 1989, pp. 281-302.

2. R. K., Shah, and A. L., London, *"Laminar Flow Forced Convection in Ducts"*, Advanced in Heat Transfer Suppi. 1, Academic Press, New York, 1978, pp. 169-176.

3. C., Berner, F., Durst, and D. M., McEligot, *"Flow Around Baffles"*, Journal of Heat Transfer, Vol. 106,1984, pp. 743-749.

4. S. V., Patanker, C.,H., Liu, and E. M., Sparrow, *"Fully Developed Flow and Heat Transfer in Ducts having Periodic Variation of the Cross-Sectional Area"*, ASME Journal of Heat Transfer, Vol. 99, 1977, pp.180-186.

5. R. L., Webb, E. R. G., Eckert, and R. J., Goldstien, *"Heat Transfer and Friction in Tubes with Repeated Rib Roughness"*, International Journal of Heat Mass Transfer, Vol. 14, 1971, pp. 601-617.

6. M. J., Lewis, *"An Elementary Analysis for Predicting the Momentum and Heat Transfer Characteristics of a Hydraulically Rough surface"*, Journal of Heat Transfer, Vol. 97, 1975, pp. 249-254.

7. C. M. B., Russel, T. V., Jones, and G. H., Lee, *"Heat Transfer Enhancement using Vortex Generators"*, The Seventh Int. Heat Transfer Conference, Vol. 3, Munchen, Fed. Rep. of Germany, 1982, pp. 283-289.

8. G., Biswas, P., Deb, and S., Biswas, *"Generation of Longitudinal Stream Wise Vortices A Device for Improving Heat Exchange Design"*, Transaction of the ASME, Vol. 16, 1994, pp. 588-597.

9. G., Biswas, and H., Chattopadhyay, *"Heat Transfer in a Channel with Built in Wing Type Vortex Generators"*, International Journal of Heat Mass Transfer, Vol. 35, No.4,1992, pp. 803-814.

10. St., Tiggeiback, N. K., Mitra, and M., Pinhig, *"Comparison of Wing Type Vortex Generators for Heat Transfer Enhancement in Channel Flow"*, Transactions of the ASME, Vol. 116, 1994, pp. 880-885.

Notations

A:	Coefficients in Eq. 7
b:	Width of the vortex genrator
B:	Width of the duct
Br:	Ratio of wing span to width of the channel = b/B
Cf:	Skin friction coefficient
Cp:	Specific heat
dh:	Hydraulic diameter
h:	Height of the duct
Nu:	Local Nusselt no.
i,j,k:	Indices, indicating positions in x, y, z directions.
k:	Thermal conductivity of the air
l:	Chord length of the wing
P:	Dimensionless pressure
Pe:	Peclet no.
Pr:	Prandtl no.
Sp:	Pressure source term
Re:	Reynolds no.
S:	Wing area
T:	Temperature
U,V, W:	Dimensionless velocities
u,v,w:	Velocities
x,y,z:	Coordinates
X, Y, Z:	Dimensionless coordinates

GREEK

α:	Aspect ratio of the channel
β:	Angle of attack
Λ:	Aspect ratio of the wing
ϕ:	General variable
μ:	Dynamic viscosity
ν:	Kinematic viscosity
θ:	Dimensionless temperature
ρ:	Density

SUBSCRIPT

1,2:	Number of grid points
in:	Inlet
ia:	Inlet of air
e,w,n,s,t,b:	Neighbors grid points